Communication

Spectroscopic Evidence for the Supply of Reactive Oxygen during CO Oxidation Catalyzed by Gold Supported on Nanocrystalline CeO

Javier Guzman, Silvio Carrettin, and Avelino Corma

J. Am. Chem. Soc., **2005**, 127 (10), 3286-3287• DOI: 10.1021/ja043752s • Publication Date (Web): 17 February 2005

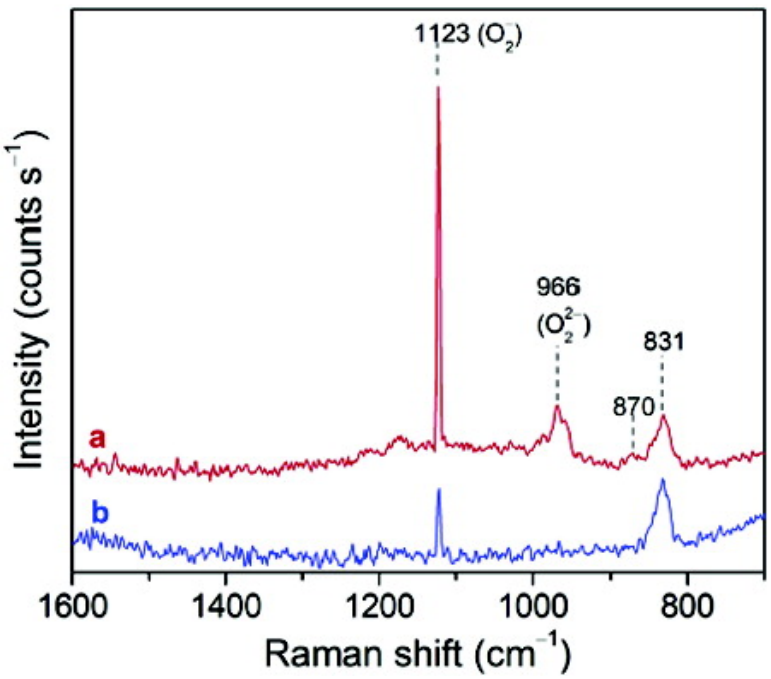

More About This Article

Additional resources and features associated with this article are available within the HTML version:

- Supporting Information
- Links to the 30 articles that cite this article, as of the time of this article download
- Access to high resolution figures
- Links to articles and content related to this article
- Copyright permission to reproduce figures and/or text from this article

View the Full Text HTML

J|A|C|S
COMMUNICATIONS

Published on Web 02/17/2005

Spectroscopic Evidence for the Supply of Reactive Oxygen during CO Oxidation Catalyzed by Gold Supported on Nanocrystalline CeO_2

Javier Guzman, Silvio Carrettin, and Avelino Corma*

Instituto de Tecnología Química, UPV-CSIC, Universidad Politécnica de Valencia, Av. de los Naranjos s/n, 46022 Valencia, Spain

Received October 14, 2004; E-mail: acorma@itq.upv.es

Highly dispersed gold supported on metal oxides is an active catalyst for several reactions,[1] including CO oxidation at low temperatures.[2] Although it is accepted that factors, such as gold particle size, synthesis method, pretreatment conditions, and support, influence the reactivity of the supported gold catalysts,[3] the nature of the active sites and the reaction mechanism for CO oxidation are still subjects of debate. In particular, the role of the support and the oxygen supply for the catalytic reaction remain controversial.[4−9] We recently reported that the characteristics of the cerium oxide surface are extremely important in determining whether a CeO_2-supported gold catalyst is active or not for CO oxidation.[10] It was found that nanocrystalline CeO_2 increases the activity of gold for CO oxidation by 2 orders of magnitude with respect to a conventionally precipitated CeO_2 support. In the present work, we report for the first time spectroscopic evidence that nanocrystalline CeO_2 supplies reactive oxygen in the form of surface η^1 superoxide species and peroxide adspecies at the one-electron defect site to the supported active species of gold for the oxidation of CO.

Nanocrystalline CeO_2 was prepared from a colloidal dispersion of CeO_2 nanoparticles (Supporting Information).[11] Gold on a nanoparticulated cerium oxide catalyst was prepared by deposition precipitation of $HAuCl_4$ using NaOH following a procedure described elsewhere.[10] The catalyst was not calcined. The total Au content of the final catalyst was 1.92 wt % as determined by chemical analysis. The catalyst was tested for CO oxidation. Expecting that the characteristics of the cerium oxide surface might affect the stabilization of different reactive gold and oxygen species, we characterized the gold catalysts prepared on nanocrystalline and conventionally precipitated CeO_2 with CO−TPR, XPS, and in situ infrared (IR) and Raman spectroscopy during CO and O_2 adsorption−reaction experiments.

IR spectroscopy characterizing CO adsorption on gold supported on nanocrystalline CeO_2 demonstrates the presence of Au^{3+}, Au^+, and Au^0 species as indicated by their characteristic Au^x−CO frequency at 2148, 2130, and 2104 cm^{-1}, respectively (Supporting Information).[8,9] An additional band was observed at 2175 cm^{-1}, which is assigned to Ce^{4+}−CO (this band was the only one observed under our experimental conditions when CO was adsorbed on nanocrystalline CeO_2). Interestingly, during CO adsorption experiments and without any oxygen in the gas stream, CO_2 was formed as indicated by the band at 2350 cm^{-1}. This result indicates that nanocrystalline CeO_2 is able to supply reactive oxygen to the gold active species for the oxidation of CO, consistent with the idea of CeO_2 acting as an oxygen buffer by releasing−uptaking oxygen through redox processes involving the Ce^{4+}/Ce^{3+} couple.[12] In contrast, when gold was deposited on precipitated CeO_2, only Au^0 (band at 2110 cm^{-1}) and a small fraction of Au^+ (band at 2135 cm^{-1}) species were detected by IR spectroscopy during CO adsorption. Furthermore, no CO_2 formation was detected during CO adsorption experiments. XPS results (Supporting Information) confirm our assignments of gold oxidation states in the Au/CeO_2 samples and provide evidence of the presence of Ce^{3+} ions on the surface of the nanocrystalline CeO_2-supported gold catalyst, consistent with previous results showing Ce^{3+} in nanocrystalline CeO_2.[13]

When O_2 was introduced in the IR cell containing a sample of gold supported on nanocrystalline CeO_2 that had been pretreated with CO, the intensity of the IR bands at 2148 and 2130 cm^{-1} decreased at a faster rate than that of the intensity of the band at 2104 cm^{-1} (Supporting Information), suggesting that although both cationic and metallic gold participate in the oxidation of CO, the catalytic active sites incorporate cationic gold, consistent with previous reports of the enhanced catalytic activity of cationic gold for CO oxidation and water−gas shift reactions.[14,15] Furthermore, the results presented in Figure 1 clearly show a direct correlation between the concentration of Au^{3+} species and catalytic activity. No correlation was found between catalytic activity and the concentration of Au^+ or Au^0 (Supporting Information).

Raman spectroscopy was used to characterize the nature of the CeO_2 support and the oxygen species formed on it. It is well established that the first-order Raman band near 464 cm^{-1} in CeO_{2-x} nanoparticles, which is assigned to the vibrational mode of the F_{2g} symmetry in a cubic fluorite lattice, shifts to lower energies, and the line shape of this feature gets broader as the particle size gets smaller.[16] Consistently, we observed this behavior when we compared the Raman spectra characterizing the conventionally precipitated (464 cm^{-1}) and nanocrystalline (457 cm^{-1}) CeO_2 supports (Supporting Information). In addition to the first-order band, a series of second-order bands were observed at 1174, 598, 422, 258, and 170 cm^{-1} (Supporting Information).

Because of the differences in crystallite size and surface properties between precipitated and nanocrystalline CeO_2, we thought that the oxygen species formed on them might be different, as well. Indeed, the Raman spectrum characterizing O_2 adsorption on conventionally prepared CeO_2 shows bands at 1314, 1361, 1408, 1428, 1470, 1527, and 1571 cm^{-1}, whereas the spectrum characterizing O_2 adsorption on nanocrystalline CeO_2 shows bands at 1123, 964, 871, and 831 cm^{-1} (Supporting Information). The band at 1571 cm^{-1} is assigned to adsorption of molecular O_2, and the bands above 1300 cm^{-1} may be assigned to $O_2^{\delta-}$ ($0 < \delta < 1$) adspecies.[17,18] The band at 1123 cm^{-1} is assigned to η^1 superoxide species.[19,20] In the peroxide range, the band at 964 cm^{-1} is assigned to peroxide adspecies at the one-electron defect site, whereas the bands at 871 and 831 cm^{-1} may be attributed to nonplanar bridging peroxide species and to the η^2 peroxide species, respectively.[17−20] These results indicate that nanocrystalline CeO_2 stabilizes O_2 as superoxide and peroxide species, whereas the conventionally precipitated CeO_2 tends to stabilize $O_2^{\delta-}$ ($0 < \delta < 1$) adspecies and molecular O_2. This might explain the enhanced reactivity of gold supported on

10.1021/ja043752s CCC: $30.25

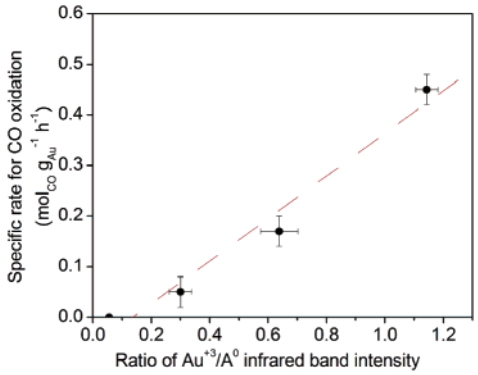

Figure 1. Correlation between Au^{3+} and Au^0 species and specific rate for CO oxidation catalyzed by gold supported on nanocrystalline CeO_2. Infrared band frequency and intensity of CO adsorption on gold catalysts were used to identify Au^{3+} (band at 2148 cm^{-1} representing $Au^{3+}-CO$) and Au^0 (band at 2104 cm^{-1} representing Au^0-CO).

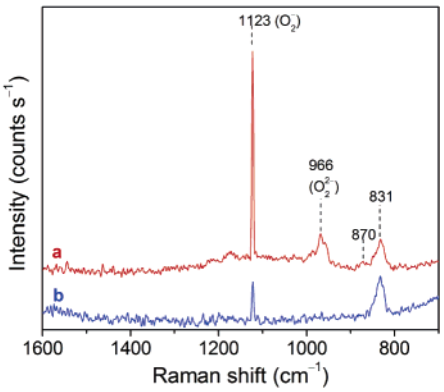

Figure 2. Raman spectra characterizing the 1.92 wt % Au/CeO_2 sample (a) at the beginning and (b) at the end of CO oxidation reaction.

nanocrystalline CeO_2 in comparison with that prepared with conventionally precipitated CeO_2.

To investigate the reactivity of the oxygen species observed on the highly active gold catalyst, a sample of gold supported on nanocrystalline CeO_2 was placed in contact with a flow of O_2 and was followed by CO + O_2 under reaction conditions. The Raman spectra characterizing the sample at the beginning and at the end of the CO oxidation are shown in Figure 2. The fresh catalyst shows Raman bands at 1123, 966, 870, and 831 cm^{-1}, which are assigned as before to η^1 superoxide species, peroxide adspecies at the one-electron defect site, nonplanar bridging peroxide species, and η^2 peroxide species, respectively.[17−20] However, when the catalyst was characterized after CO oxidation, the intensity of the Raman band at 1123 cm^{-1} decreased and the band at 966 cm^{-1} disappeared, indicating the involvement of η^1 superoxide species and peroxide adspecies at the one-electron defect site in the oxidation of CO. Furthermore, the results provide evidence that nonplanar bridging peroxide species, η^2 peroxide species, molecular oxygen, or lattice oxygen do not participate in the direct oxidation of CO, consistent with postulated CO oxidation mechanisms.[3,4,10,20] Our results infer that cationic gold is stabilized on nanoparticulated CeO_2 by creating Ce^{3+} and oxygen vacancy sites, where peroxide species could be eventually formed for the oxidation of CO.

Results of CO−TPR confirm the oxidation of CO to CO_2, even at room temperature, and the participation of four different surface oxygen species with different operating conditions (Supporting Information). The high-temperature oxygen species (548 °C) are associated with lattice oxygen, which do not participate in the catalytic oxidation of CO at low temperatures.[15] The oxygen species with a maximum uptake at 113 and 201 °C may be attributed to surface oxygen species (superoxide and peroxide adspecies, respectively), in agreement with Raman results.[15] Furthermore, cyclic TPR experiments (Supporting Information) demonstrate the regeneration of the gold active sites during reduction and oxidation of the catalyst.

In summary, the data demonstrate that both cationic and metallic gold are present in the gold catalyst prepared with nanocrystalline CeO_2, and that the catalytic active sites incorporate cationic gold. Nanocrystalline CeO_2 stabilizes O_2 as superoxide and peroxide species, whereas the precipitated CeO_2 tends to stabilize $O_2^{\delta-}$ and molecular O_2. Furthermore, nanocrystalline CeO_2 supplies reactive oxygen in the form of surface η^1 superoxide species and peroxide adspecies at the one-electron defect site to the supported active species of gold for the oxidation of CO.

Acknowledgment. This research was supported by the Spanish CICYT (MAT 2003-07945-C02-01) and the Auricat EU network (HPRN-CT-2002-00174).

Supporting Information Available: Experimental details and additional results. This material is available free of charge via the Internet at http://pubs.acs.org.

References

(1) (a) Nkosi, B.; Adams, M. D.; Coville, N. J.; Hutchings, G. J. *J. Catal.* **1991**, *128*, 333. (b) Carrettin, S.; McMorn, P.; Johnston, P.; Griffin, K.; Hutchings, G. J. *Chem. Commun.* **2002**, *7*, 696. (c) Guzman, J.; Gates, B. C. *Angew. Chem., Int. Ed.* **2003**, *42*, 690.
(2) (a) Haruta, M.; Kobayashi, T.; Sano, H.; Yamada, N. *Chem. Lett.* **1987**, 405. (b) Haruta, M.; Yamada, N.; Kobayashi, T.; Iijima, S. *J. Catal.* **1989**, *115*, 301.
(3) (a) Hutchings, G. J. *Gold Bull.* **1996**, *29*, 123. (b) Bond, G. C.; Thompson, D. T. *Catal. Rev. Sci. Eng.* **1999**, *41*, 319.
(4) Schubert, M. M.; Hackengerg, S.; van Veen, A. C.; Muhler, M.; Plzak, V.; Behm, R. J. *J. Catal.* **2001**, *197*, 113.
(5) Guzman, J.; Gates, B. C. *J. Am. Chem. Soc.* **2004**, *126*, 2672.
(6) Kung, H. H.; Kung, M. C.; Costello, C. K. *J. Catal.* **2003**, *216*, 425.
(7) Davis, R. J. *Science* **2003**, *301*, 926.
(8) (a) Boccuzzi, F.; Chiorino, A.; Tsubota, S.; Haruta, M. *J. Phys. Chem.* **1996**, *100*, 3625. (b) Boccuzzi, F.; Chiorino, A.; Manzoli, M.; Lu, P.; Akita, T.; Ichikawa, S.; Haruta, M. *J. Catal.* **2001**, *202*, 256.
(9) (a) Liu, H.; Kozlov, A. I.; Kozlova, A. P.; Shido, T.; Iwasawa, Y. *Phys. Chem. Chem. Phys.* **1999**, *1*, 2851. (b) Liu, H.; Kozlov, A. I.; Kozlova, A. P.; Shido, T.; Asakura, K.; Iwasawa, Y. *J. Catal.* **1999**, *185*, 252. (c) Guzman, J.; Corma, A. *Chem. Commun.* **2005**, *6*, 743.
(10) Carrettin, S.; Concepción, P.; Corma, A.; López Nieto, J. M.; Puntes, V. F. *Angew. Chem., Int. Ed.* **2004**, *43*, 2538.
(11) Chane-Ching, J. Y. EP208580, 1987.
(12) Trovarelli, A. *Catal. Rev. Sci. Eng.* **1996**, *38*, 439.
(13) Zhang, F.; Wang, P.; Koberstein, J.; Khalid, S. K.; Chan, S.-W. *Surf. Sci.* **2004**, *563*, 74.
(14) Guzman, J.; Gates, B. C. *J. Phys. Chem. B* **2002**, *106*, 7659.
(15) Fu, Q.; Saltsburg, H.; Flytzani-Stephanopoulos, M. *Science* **2003**, *301*, 935.
(16) Spanier, J. E.; Robinson, R. D.; Zheng, F.; Chan, S. W.; Herman, I. P. *Phys. Rev. B* **2001**, *64*, 245407.
(17) Long, R. Q.; Huang, Y. P.; Wan, H. L. *J. Raman Spectrosc.* **1997**, *28*, 29.
(18) Long, R. Q.; Wan, H. L. *J. Chem. Soc., Faraday Trans.* **1997**, *93*, 355.
(19) Li, C.; Domen, K.; Maruya, K.-I.; Onishi, T. *J. Catal.* **1990**, *123*, 436.
(20) Pushkarev, V. V.; Kovalchuk, V. I.; d'Itri, J. L. *J. Phys. Chem. B* **2004**, *108*, 5341.

JA043752S